Two Dimensional Imaging of Model Targets with a CW Radar

Uve H. W. Lammers, Richard A. Marr, and John B. Morris

Rome Laboratory*

ABSTRACT

Single-frequency operation is desirable for an instrumentation radar intended for target scattering and imaging studies. Simplicity and the high resolution achievable with Doppler information alone make it attractive. We have developed a technique for two dimensional imaging based on a unique form of target motion. The target precesses around a spatially fixed axis, similar to a rotating mechanical top, except that the target does not rotate. The Doppler shift observed by a CW radar, positioned along the precession axis, yields high resolution images. Aspect angle and polarization dependence as well as shadowing, which are problems with other imaging methods, can be minimized. The soundness of the technique is demonstrated experimentally at 140GHz.

INTRODUCTION

Precessional target motion provides a means of producing two dimensional images of that target with a stationary CW radar. This technique is ideally suited where the generation of a wideband waveform for ranging is difficult or impossible for the radar, and where it is relatively easy to impose precessional motion on the target. This is the case when imaging model targets at short millimeter and submillimeter wavelengths. Models may be scaled versions of full-size targets with the radar wavelength also scaled to simulate a real-world situation. Or they may be generic targets to study scattering phenomena on conveniently manufactured and manipulated geometrical bodies or composites thereof. It will be seen that precessional target motion provides two dimensional resolution commensurate with model-size targets and superior to what is achievable with conventional wideband waveforms. Precessional target motion requires a highly cooperative target and is thus usable in a laboratory setting only. The degree of phase coherence necessary for the desired resolution presents a major challenge with this imaging technique, especially at millimeter and submillimeter wavelengths. In a short-range indoor system compensation methods can be used to achieve the required coherence with relative simplicity.

1. SCATTERING GEOMETRIES

Radar targets of interest here typically represent arrangements of more or less specular point scatterers. In conventional Doppler imaging, a two dimensional target in the x,y plane (upper half of Figure 1) rotates around the z axis. The signal returned by scatterer $g(r, \psi)$ toward a CW radar looking in the positive y direction exhibits a phase progression or Doppler shift as a function of target rotation angle θ, which is unique to its r ψ, location. This holds accordingly for other scatterers contained within the target boundary. The inverse Fourier transform of the sum signal $G(\theta)$ received by the radar from all scatterers as a function of θ is the image of that target (Mensa, 1990)

$$g(r,\psi) = 2/\lambda \int_0^{2\pi} G(\theta) \exp\left[(-j\, 4\, \pi\, r/\lambda) \cos(\theta + \psi) \right] d\theta \,. \quad (1)$$

The positive sign in the cosine term results from our choice of reference.

For a point scatterer to yield a circularly symmetric image (or point spread function) θ must cover a range of 2π. This requires isotropic scatterers such as spheres and cylinders and leads to shadowing in a multiscatterer target. Because of their concentric sidelobes of considerable magnitude, interference between point spread functions of multiple scatterers on a target quickly leads to a cluttered image. Vector addition of images obtained at different

* RL/ERCP, Hanscom Air Force Base, Massachusetts, 01731 USA.

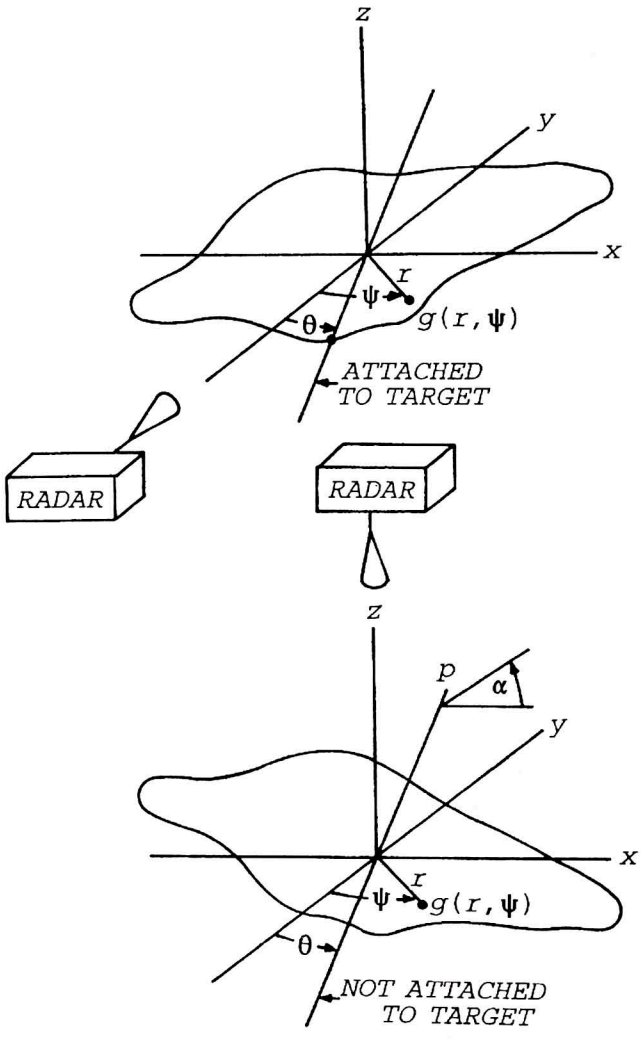

Fig. 1 - Top: rotation geometry, bottom: precession geometry.

wavelengths λ is necessary to satisfactorily image a target with multiple scatterers.

Multiwavelength measurements are not easily implemented at short millimeter and submillimeter wavelengths. We have, therefore, developed the imaging method shown in the lower half of Figure 1. The radar now looks in the negative z direction. The target, while still in the x,y plane, no longer rotates. It tilts by an angle α around the p axis, which is in the x,y plane. Except for points along the p axis, the target leaves the x,y plane. The tilt axis p is rotated in the x, y plane in increments of θ. At each angular position of the p axis the target is tilted by the same angle α. The axis of target tilt, not the target itself, rotates around the z axis. The resultant sequence of target positions represents a stepwise precession. Thus, for a fixed α, the target's distributed scatterers return to the radar component signals, whose individual phases change with the direction of the p axis and their specific x,y location on the target. It can be shown (Lammers and Marr) that the inverse Fourier transform of the sum signal $G(\theta)$ thus obtained also yields the image of the target

$$g(r,\psi) = 2 \sin\alpha/\lambda \int_0^{2\pi} G(\theta) \exp [(-j\, 4\pi r \sin\alpha/\lambda) \sin(\theta - \psi)]\, d\theta. \quad (2)$$

The image at a single λ and α suffers from the same sidelobe interference problem in a multiscatterer target as the one generated by the rotating-target method. However, vectorial superposition of multiple images of constant λ and different α leads to sidelobe cancellation as before, even with a CW radar. There are further advantages to this imaging technique. The rotating-target method yields a resolution of 0.2 λ (3dB width of point spread function, Mensa, 1990). The precessing-target-method resolution is $0.2\,\lambda/\sin\alpha$. At 140GHz ($\lambda = 2.14mm$) and $\alpha = 10\ deg$ this translates to 0.43mm for rotation and 2.46mm for precession. If one assumes the range resolution of a wideband waveform as s = c / (2b), where c is the velocity of light and b is the bandwidth, then 2.46mm resolution corresponds to a 60.9GHz bandwidth. Such bandwidth is very difficult if not impossible to achieve. Further advantages of the precessing- target method are obvious. For $\alpha = 10\ deg$, angle independent scattering from the target is required over a range of only 20deg (i. e. +/- α), not 360deg. Polarization constraints are eased correspondingly. A two dimensional target experiences no shadowing for $\alpha < 90\ deg$.

2. PHASE STABILIZATION

Experimental imaging of a precessing target typically involves measurement of $G(\theta)$ at 50 equispaced θ positions and fixed α. Angle α is changed parametrically from 0 to α_{max} in 16 steps, such that the sin α increment is kept constant. This results in 800 measurements of 5 seconds each, a considerable time over which phase coherence between measurements has to be maintained. Figure 2 shows diagrammatically how this is accomplished. Power from a single millimeter or submillimeter wave source is divided into two components. One component is Doppler shifted in frequency by a mechanically rotating frequency shifter or single-sideband modulator before transmission. The other component is left unshifted for use as a first local oscillator (LO) signal. Under the condition of only a small differential delay between transmit and LO paths, most frequency and phase instabilities of the source are eliminated in the process of forming a first intermediate frequency (IF). This condition is easily met using an unstabilized source like a Gunn oscillator in an indoor radar range. The IF is directly proportional to frequency shifter rotation rate N, however. Motor speed fluctuations

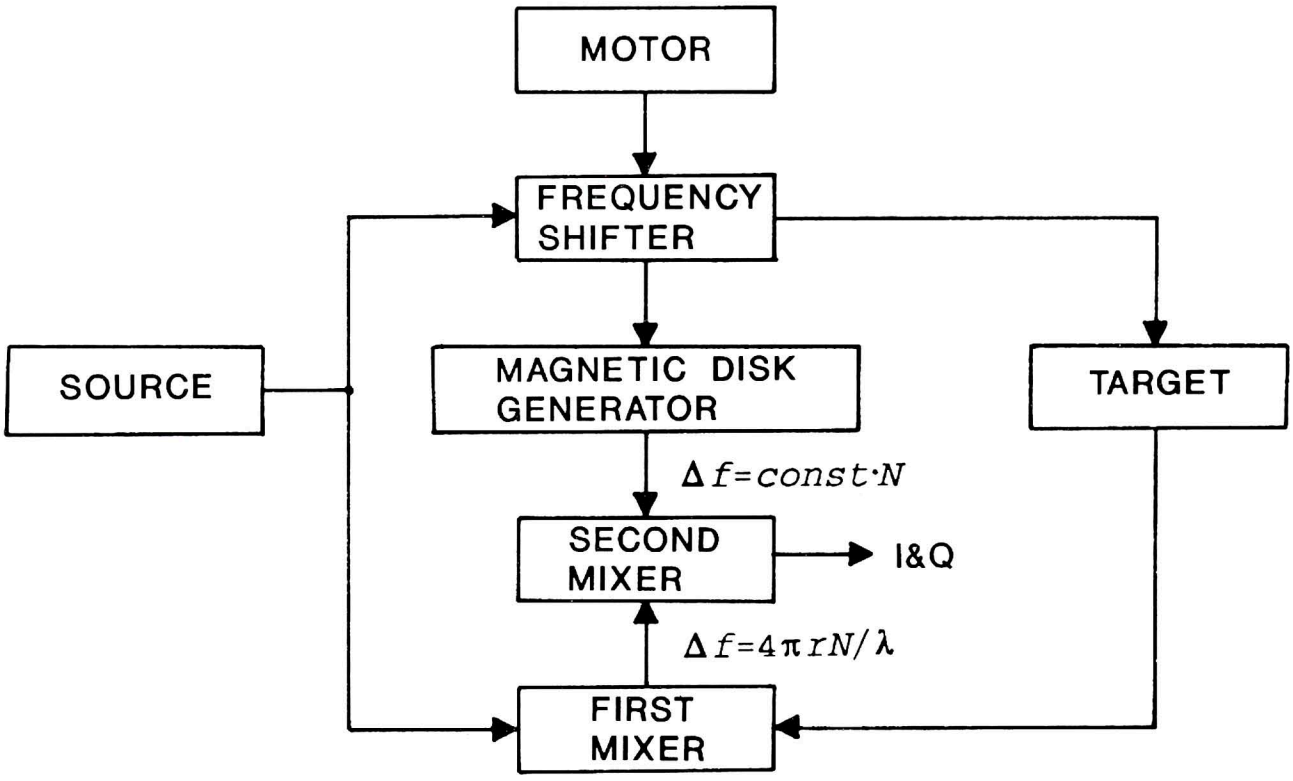

Fig. 2 - Phase stabilization scheme.

would be indistinguishable from target induced Doppler shifts. The first IF from a strong, stationary target is, therefore, first recorded magnetically on a disk that is rigidly attached to the central rotating cylinder of the frequency shifter (Figure 3). During the measurement of an actual precessing target, the magnetically recorded waveform is read from the disk and used to generate a second LO signal to downconvert target phase information to baseband in-phase and quadrature components. Since both first IF and second LO frequencies are proportional to N, variations in N are eliminated in the second mixing process.

4. MEASUREMENT SYSTEM

The mechanical frequency shifter in Figure 3 is a quasioptical device, originally designed for submillimeter wave application but usable at shorter millimeter wavelengths as well. The Gaussian beam approaches from the right in a direction orthogonal to the base plate. It is deflected by two flat mirrors mounted inside the central rotating aluminum cylinder (behind the darker magnetic disk), first radially and then tangentially with the aluminum cylinder. The beam then retroreflects from one of four stationary reflectors, which in the plane of beam motion are shaped according to the involute of a circle. The circle radius is the rotation radius of the outer flat mirror (Lammers, Marr, and Morris, 1990). The beam leaves the shifter on the same path on which it entered. The phase progression of the retroreflected signal as a function of rotation angle is linear until a phase jump of an integer number of wavelengths occurs as the beam transitions from one to the next stationary reflector. This results in a highly monochromatic frequency transposition. The magnetic write/read head is visible in front of the upper left portion of the magnetic disk.

The complete 140GHz imaging radar can be seen in Figure 4. It is a waveguide system except for the mechanical frequency shifter in the left foreground. The shifter is fed by a signal launched from the circular feed horn and focussed by a dielectric lens (partially hidden by the elliptical plate). The radar antenna proper is a rectangular feed horn. The radar signal propagates horizontally forward and is then deflected downward by the flat elliptical plate, mounted at 45deg relative to the beam. The target (three metal spheres in the figure) is supported by a foam tripod. The tripod is suspended from three thin threads, which on their upper end wind onto the shafts of three stepper motors. The stepper motors are computer control-

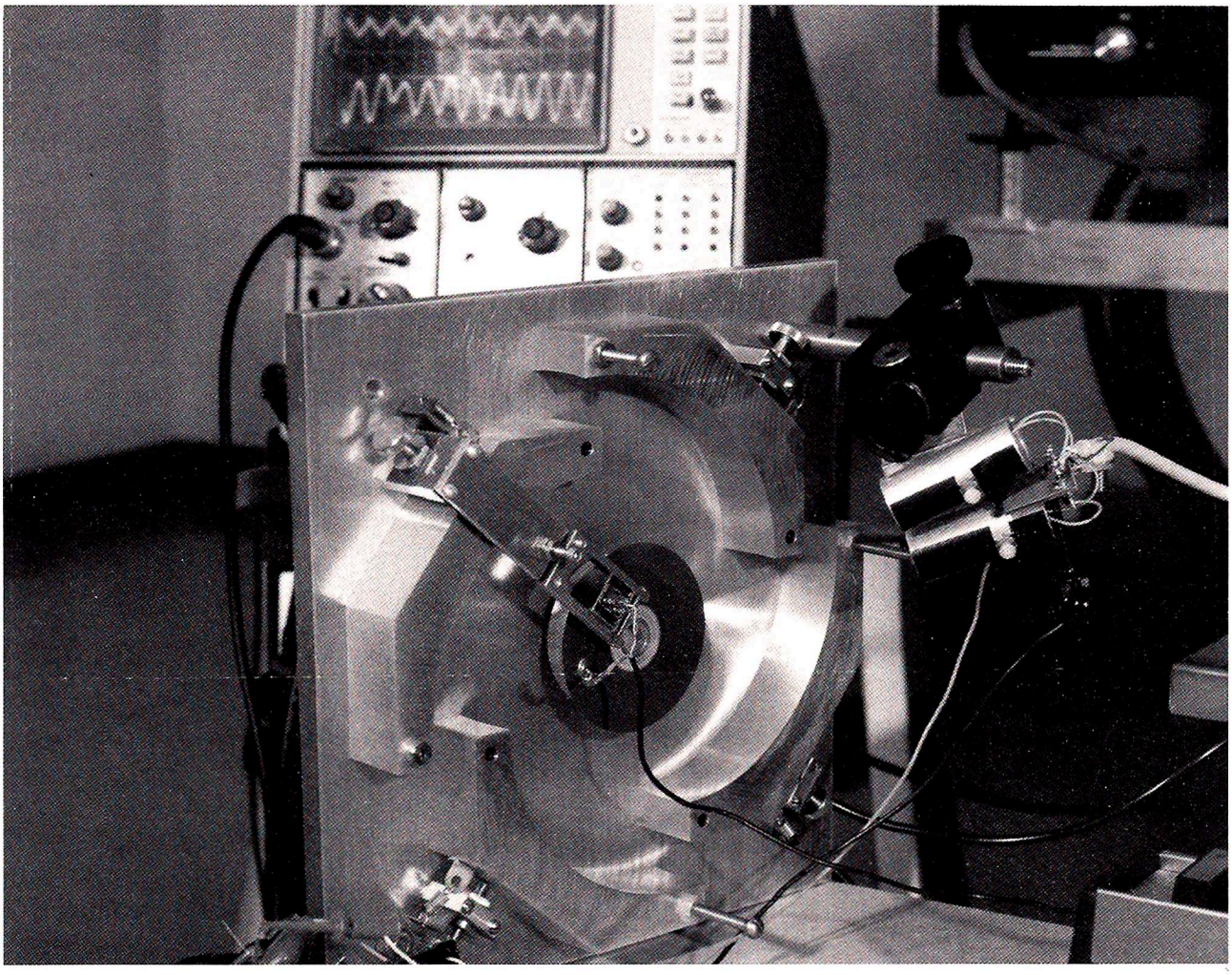

Fig. 3 - Mechanical frequency shifter (radar detail).

led in such a fashion that by individually lengthening and shortening the threads the target performs a precessional motion. The target is in the antenna far field. Minor lateral sway due to the thread support is largely inconsequential. Radar energy bypassing the target is deflected by the obliquely mounted wood plate underneath. The whole motor/reflector/target support structure is made of wood. A complete block diagram containing the various features discussed so far is seen in Figure 5. Transmit/receive signal discrimination in the single- radar-antenna configuration is accomplished by a hybrid ring, which is carefully balanced by an EH tuner inserted between isolator and hybrid ring. Source and motor drive generator are unstabilized. The target is shown on a computer controlled turntable, a feature that relates to the rotating-target method. The magnetically read signal is actually used to phaselock the second LO.

5. EXPERIMENTAL IMAGES

The triple-sphere target in Figure 4 is imaged in Figure 6. The top row shows topographic displays, the bottom row shows perspective displays. The image field is 48 by 48 wavelengths in all cases. Image magnitude in the top row is coded in contour line density and in the bottom row as vertical height. The maximum *slphs* of 10deg was divided into 16 increments as mentioned before with the inner four images (smallest α) vectorially added shown on the left, the inner eight adjacent, the inner twelve next, and all sixteen on the right. An artifact, originally overlooked, provides an interesting demonstration of the operation of precession based imaging. The ball bearing spheres of 11.9, 6.4, and 5.6mm diameter were attached to the foam tripod with rectangular pieces of doublesided adhesive tape to prevent them from rolling off. These more or less

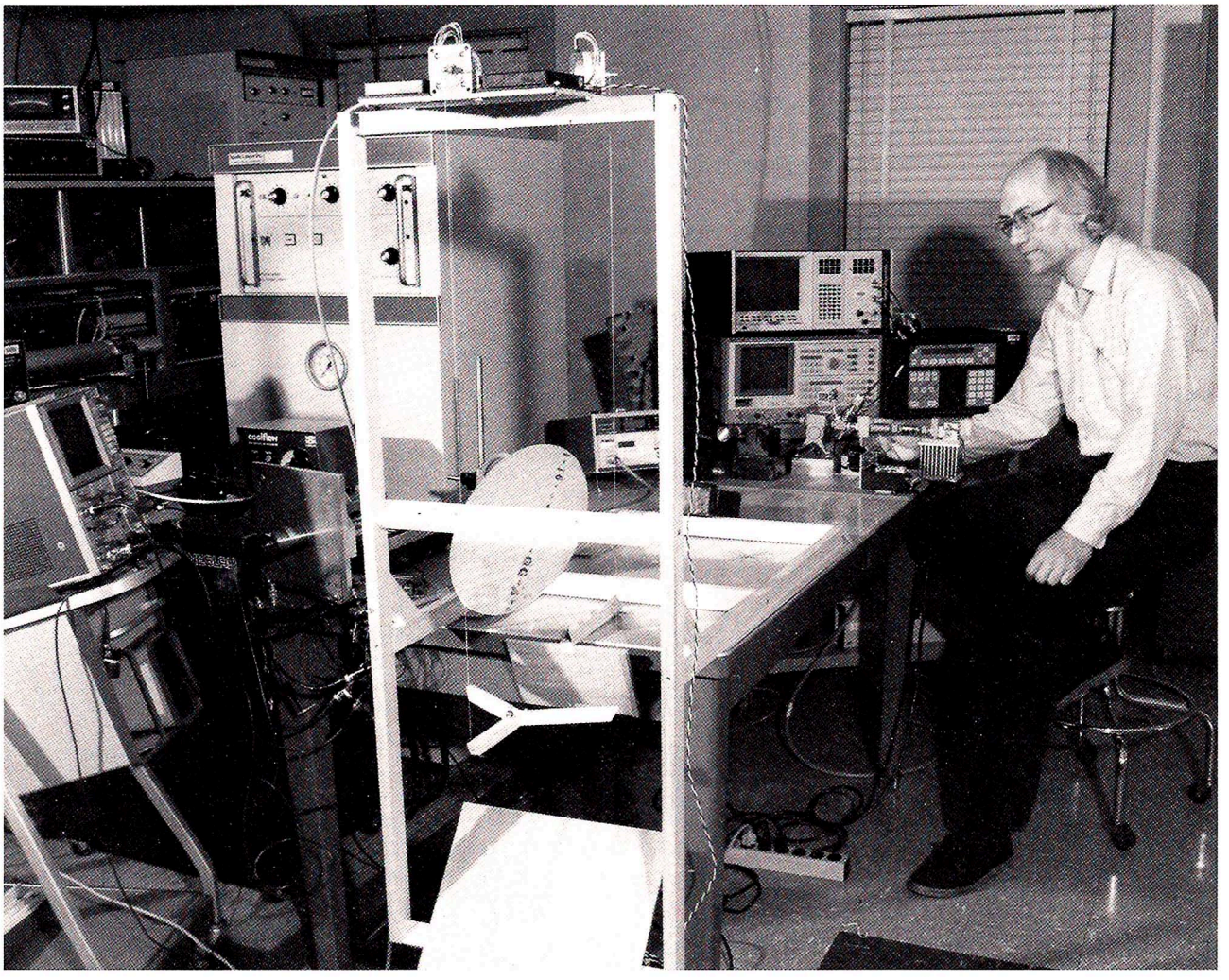

Fig. 4 - 140GHz imaging CW radar.

flat pieces of tape constitute specular reflectors at small α with returns comparable to those of the metal spheres. The leftmost column of images shows mostly the tape pieces at a resolution commensurate with the small α involved. In the next column separate returns from tape pieces and spheres become more apparent. These returns are not necessarily co-located. The tape outlines are somewhat delineated. The third set of images displays the correct locations of the spheres and their positions relative to the well delineated tape pieces. The final set of images is dominated by the sphere returns. The α tilt is so large now that the tape reflection is directed away from the radar antenna and does not add to the vector sum any more. A discrepancy remains unexplained. The return from the 5.6mm sphere exceeds that of the 6.4mm sphere. This is not in agreement with Mie theory (Skolnik,1970).

A toy antique model car is imaged in Figure 7. The length of the model is 76mm. This is a three dimensional target. It can be shown that for small α ($\alpha \leq 10\ deg$) the three dimensional point spread function is narrow in x and y directions and wide in z direction. That is, a three dimensional target images essentially in a plane. This is the case in Figure 7, which presents a fairly recognizable image of the car without a contour overlay. The hood, windshield, and seat are visible. The wheels, also reasonably placed and shaped, are probably more narrowly constrained scatterers (perhaps the hubs), which the limited x,y resolution due to $\alpha = 5\ deg$ has expanded to fullsize structures.

The informal RL logo in Figure 8 is a two dimensional metallic target. At a height of 83mm its beam of re-radiation must be narrow in most planes at this wavelength. To make it a more "diffuse" target, its surface was dimpled in a semiregular fashion. Note the high resolution of the image at $\alpha = 10\ deg$. It agrees qualitatively with the theoretical value of 2.46mm computed for this wavelength and this tilt angle. The topographic image in Figure 8 conceals the spiky nature of the image to some extent. We are investigating the latter characteristic.

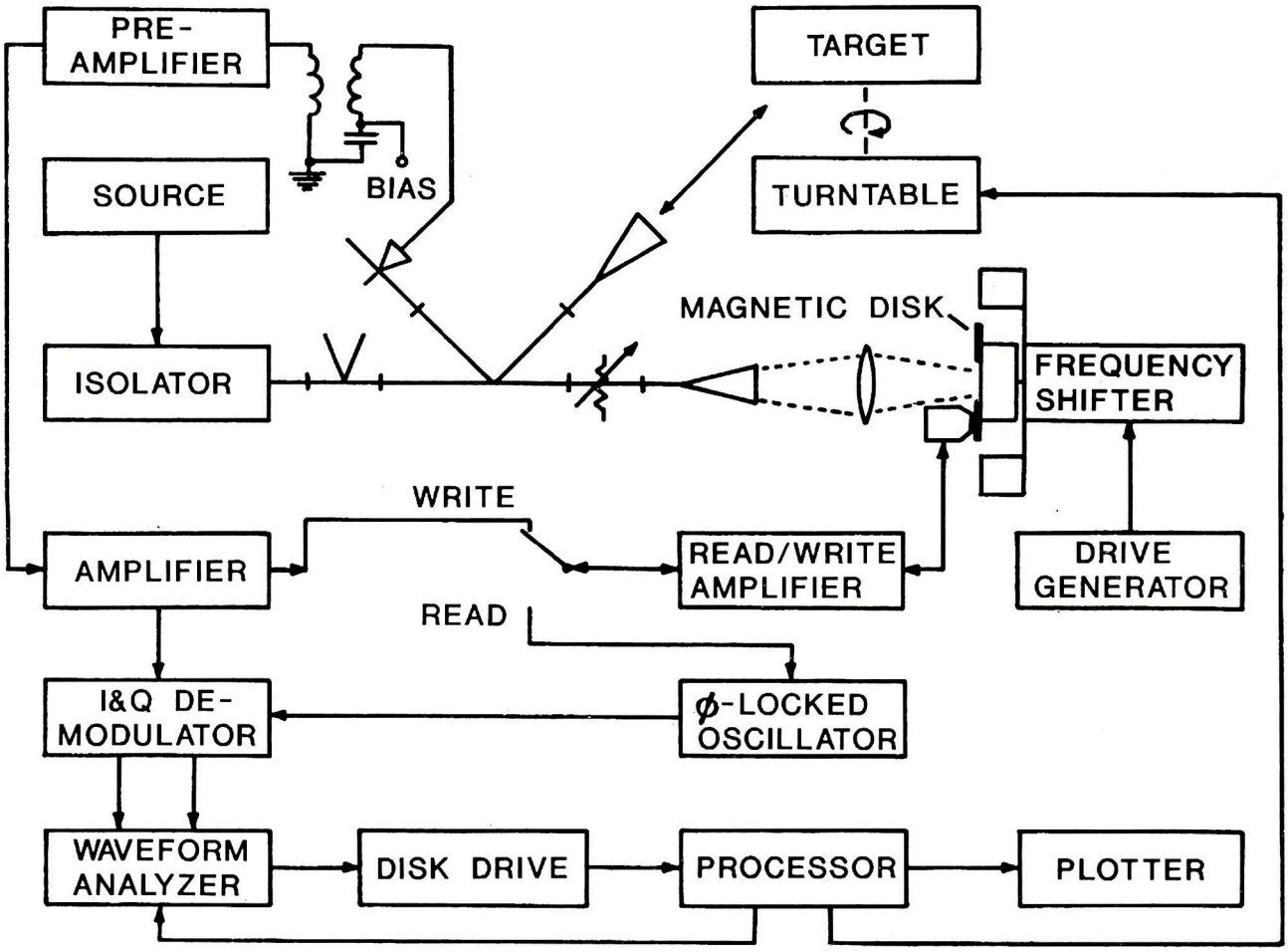

Fig. 5 - Radar block diagram.

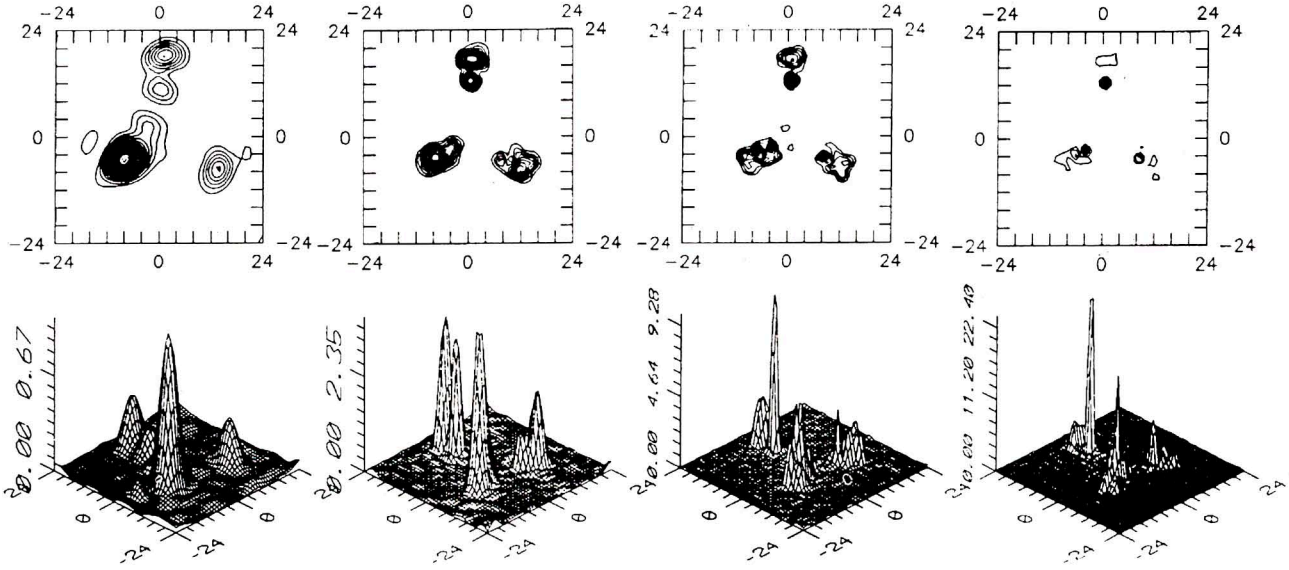

Fig. 6 - Vectorially superimposed images of triple metallic spheres with sin α = n (sin 10)/16 ; n = 1 to 4 on left, n = 1 to 16 on right.

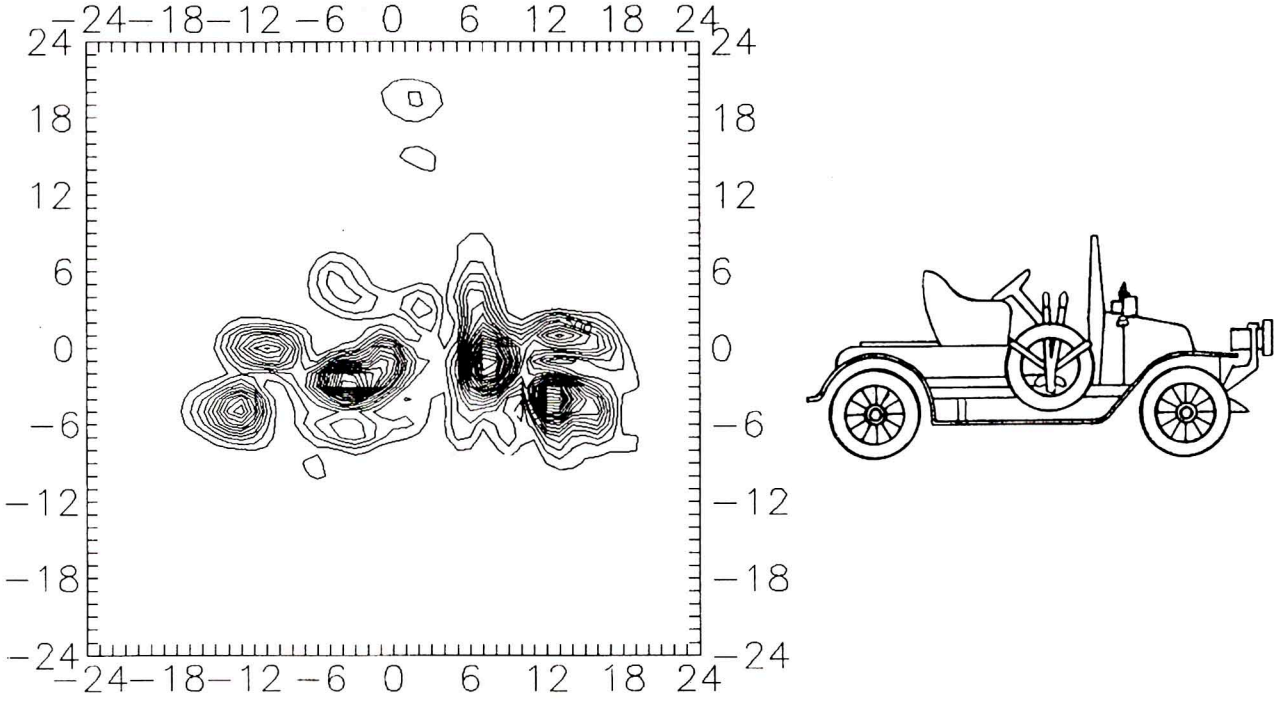

Fig. 7 - Image (left) and line drawing (right) of toy model car (length 76mm); image field 48 by 48 wavelengths (λ = 2.14mm).

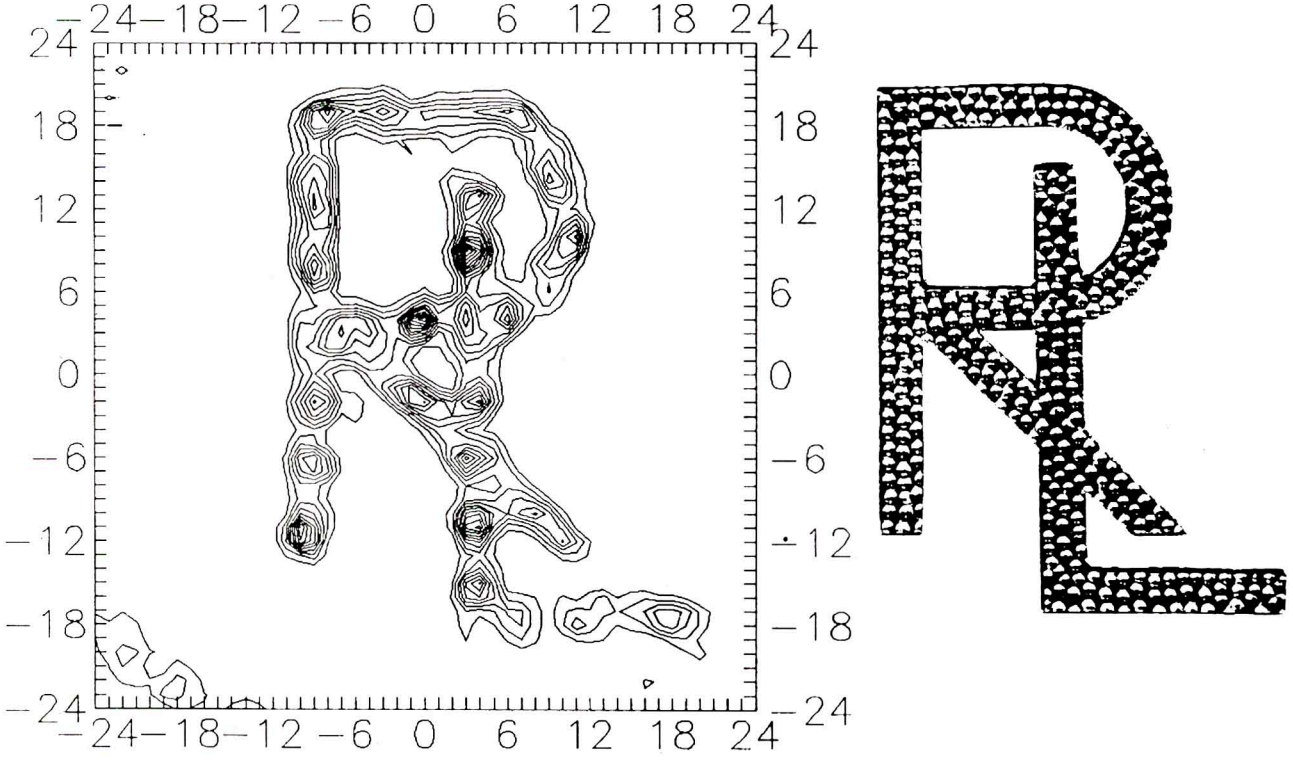

Fig. 8 - Image (left) and photo copy (right) of two dimensional metallic RL logo (height 83mm); image field 48 by 48 wavelengths (λ = 2.14mm).

CONCLUSION

It is apparant that imaging of a precessing target with a CW radar is an efficient tool to study electromagnetic scattering phenomena. The extremely high resolution in two dimensions compared with practical ranging systems makes possible the use of model-size targets with their advantage in cost and ease of handling. As described, precessing-target images are in a plane different from the one of a pulse-Doppler imaging radar. The precessing-target method is truly monochromatic. This has implications in terms of target resonances. It is not monodirectional, however, and backscatter directivity has to be taken into consideration. We have only addressed precession based imaging with the radar looking in the negative z direction and with a small α. Two dimensional imaging on this basis is also possible with the radar looking in x or y direction or in any other direction relative to the precession axis. Larger α values permit three dimensional imaging.

REFERENCES

Lammers, U. H. W., Marr, R. A., and Morris, J. B., 1990, A coherent mechanical submillimeter frequency shifter, Int. J. IR and MM Waves, 11, 367.

Lammers, U. H. W. and Marr, R. A., Doppler imaging based on radar target precession, IEEE Trans. AES, accepted for publication.

Mensa, D. L., High Resolution Radar Cross-Section Imaging (Boston: Artech House).

Skolnik, M. I., Radar Handbook (New York: McGraw Hill).